Convective particle transport arising from poloidal inhomogeneity in tokamak *H* mode

N. Kasuya[a] and K. Itoh
National Institute for Fusion Science, Toki, Gifu 509-5292, Japan

(Received 7 April 2005; accepted 5 July 2005; published online 21 September 2005)

In tokamak high-confinement modes (*H* modes), a large poloidal flow exists within an edge transport barrier, and the electrostatic potential and density profiles can be steep both in the radial and poloidal directions. The two-dimensional structures of the electrostatic potential, density, and flow velocity near the edge of a tokamak plasma are investigated. The analysis is carried out with the momentum conservation law using the shock ordering. For the case with a strong radial electric field (*H*-mode case), a particle flux is induced from asymmetry of the poloidal electric field in the transport barrier. This convective transport is found to depend weakly on collisionality, and changes its direction in accordance with the direction of the radial electric field, the toroidal magnetic field, and the plasma current. The divergence of a particle flux is a source of temporal variation of the density, and there are negative divergence regions both in the inward and outward flux cases. Thus this convective particle flux is a new candidate for the cause of the rapid establishment of the density pedestal after the onset of low to high confinement mode (*L*/*H*) transition. © *2005 American Institute of Physics*. [DOI: 10.1063/1.2034347]

I. INTRODUCTION

Toroidal plasmas have nonlinear response, which allows a variety of structures to be formed.[1] In particular, the formation of transport barriers in high-confinement mode (*H* mode) toroidal plasmas[2] has been the focus of numerous researches. Key mechanisms to understand the *H*-mode transition include bifurcation of the electric field[3,4] and the associated suppression of turbulence by electric-field structures.[5,6] Thus significant attention has been devoted to studying the steep radial electric-field structure in the low to high confinement mode (*L*/*H*) transition physics.[7]

The previous *H*-mode studies have been mainly carried out to clarify the detailed structural formation mechanisms in the radial direction. For example, the nonlinear structural formation mechanism of the radial electric field has been studied with biased limiter experiments in which an externally driven *H*-mode transition was induced.[8,9] An externally imposed voltage changes the radial electric-field structure in the same way as in spontaneous *H* modes. This forced transition is characterized by a sudden change of the radial electric-field structure from a flat one to a peaked one. Theoretical studies have clarified the formation mechanism of this solitary radial electric-field structure.[10,11] The radial electric-field structure is calculated from the charge conservation law,

$$\frac{\partial}{\partial t}E_r = -\frac{1}{\varepsilon_0 \varepsilon_\perp}(J_{\mathrm{visc}} + J_r - J_{\mathrm{ext}}), \tag{1}$$

where E_r is the radial electric field, J_{visc} is the current driven by shear viscosity, J_r is the local current, J_{ext} includes the current driven into the electrode by the external circuit and ion orbit loss current, etc., ε_0 is the vacuum susceptibility, and $\varepsilon_\perp$ is the dielectric constant of a magnetized plasma. The nonlinearity of the local current has a major effect on structural bifurcation of the radial electric field. The radial electric-field structure has a large gradient, which is typical in *H* modes. The nonlinearity in the relationship between the radial electric field and the radial current has been examined explicitly in other toroidal plasma experiments.[12]

Although significant progress has been made in clarifying the radial electric-field structure, several fundamental issues still remain. For instance, the existence of a poloidal shock structure associated with a large poloidal flow has not been clarified. The poloidal shock is a steady density or potential jump in the poloidal direction. In *H* modes, a large radial electric field in a transport barrier makes a large $E \times B$ flow pointing in the poloidal direction. The poloidal Mach number $M_p = E_r/(v_{ti}B_p)$ is large enough to exceed unity in the *H* mode, where $v_{ti} = \sqrt{2T_i/m_i}$ is the thermal velocity of ions, T_i is the ion temperature, m_i is the ion mass, and B_p is the poloidal magnetic field. In theoretical studies, in which only the poloidal variation was taken and the radial structure was neglected, it was predicted that the poloidal shock can appear in *H*-mode plasmas.[13,14] In Ref. 13 the poloidal shock structure in a single magnetic-flux surface is derived from the momentum balance equation. The flow is compressible with a supersonic poloidal flow, so the convective derivative term becomes effective in forming the shock structure. The shock position depends on M_p, so as the poloidal flow increases, the shock position changes correspondingly. The maximum gradient in the poloidal direction is given at the shock position. It can be explained that the poloidal shock is formed in the case when the subsonic and supersonic states are both exist, and the shock appears at the boundary between these regions.[15]

The existence of a steep structure both in the radial and poloidal directions suggests the importance of two dimen-

[a]Electronic mail: kasuya@nifs.ac.jp

sionality in H modes. Analysis of two-dimensional velocity and density profiles has been carried out in Ref. 16, in which only the low-order Fourier components were taken into account. Poloidal shock in the two-dimensional structure has been under consideration.[15] Some experiments have indicated poloidal asymmetry.[17,18]

It is well known that turbulent diffusivity decreases rapidly after transition.[7,19] However, this reduced diffusion makes the time required to reach a steady state much longer than observed, which contradicts to the observation of the rapid establishment of the density profile pedestal after the onset of L/H transition.[20] One possible cause of the rapid establishment of the pedestal is the increase of a particle convective flux.[21] There are many theories to explain the inward pinch,[22–26] but its origin has yet to be unresolved. A large poloidal electric field is localized at the shock position, which generates a convective $E\times B$ flow in the radial direction.[1] This convective transport is a candidate for the cause of the rapid establishment of the pedestal, because it increases right after the onset of L/H transition.

In this paper, we study the two-dimensional structure of the electrostatic potential, density, and flow velocity near the edge of a tokamak plasma. A set of equations, which describes the transition to the steep radial electric-field structure as well as the poloidal inhomogeneity, is derived by considering the nonlinearity in bulk-ion viscosity and (turbulence-driven) shear viscosity. By introducing an ordering (shock ordering[13]), the coupled nonlinear partial differential equations are divided into two parts. The first is an ordinary differential equation that governs the steep radial structure of the radial electric field (or poloidal flow). The bifurcation and transition of the poloidally averaged part of the radial electric field are obtained from this equation. The second is a nonlinear partial differential equation that governs the poloidal asymmetry of the flow (including the poloidal shock). In the latter equation, the radial structure of the strong radial electric field is already given by the former equation. Thus the theoretical framework that describes the bifurcation of the radial structure as well as poloidal inhomogeneity is obtained. It is emphasized that the validity of the L/H transition theory, which has been based upon the one-dimensional analyses, is confirmed by this two-dimensional analysis. The two-dimensional structure generates the particle flux in the radial direction, whose magnitude is not constant in space. Thus the divergence of this convective flux induces temporal variation of the density, inducing the edge pedestal rapidly after the onset of L/H transition.

The paper is organized as follows. Derivation of the model equations is described in Sec. II. In Sec. III, solutions of two-dimensional structures are described, corresponding to the onset of the L/H transition. The flux-surface-averaged convective flux by the $E\times B$ flow pointing in the radial direction is calculated to estimate the effect of the two-dimensional structure in Sec. IV. Effect of collision and direction of the convective flux with the inversion of the sign of plasma parameters are examined in Secs. V and VI, respectively. Its effect on the formation of the edge transport barrier is discussed in Sec. VII.

II. MODEL EQUATION

A. Geometry and momentum balance for the two-dimensional problem

To evaluate the two-dimensional structure in tokamak edge plasma, the flux-surface-averaged equations are inappropriate. We consider a large aspect ratio tokamak with a circular cross section, and the coordinates (r,θ,ζ) are used (r: radius; θ: poloidal angle; ζ: toroidal angle). Poloidal variations of the density and the electrostatic potential are considered, but that of the temperature is neglected. Electrons are isothermal, ions are adiabatic, and $n_i=n_e\equiv n$ is assumed, where n_i and n_e are the ion and electron densities, respectively. The derivation of the model equation follows Ref. 13, but the radial flow and shear viscosity are taken into account here.[27] By these terms, the radial and poloidal structures are coupled with each other. The structures are governed by the momentum balance equation

$$m_i n\frac{d}{dt}\mathbf{V}_i=\mathbf{J}\times\mathbf{B}-\boldsymbol{\nabla}(p_i+p_e)-(\boldsymbol{\nabla}\cdot\overleftrightarrow{\pi}_i)_{\mathrm{bulk}}-(\boldsymbol{\nabla}\cdot\overleftrightarrow{\pi}_i)_{\mathrm{shear}},\tag{2}$$

where $\mathbf{V}_i$ is the flow velocity, $\mathbf{J}$ is the plasma current, p_i and p_e are the ion and electron pressures. Pressure $p=nT$, and constant temperature T is assumed. The viscosity $\overleftrightarrow{\pi}_i$ is divided into two terms: bulk viscosity given by a neoclassical process,[28] and shear viscosity given by an anomalous process.[1] The viscosity of electrons is neglected because it is smaller by a factor on the order of $\sqrt{m_e/m_i}$. The perpendicular flow is given by the $E\times B$ drift here, and the flow velocity is written as

$$\mathbf{V}=\mathbf{V}_{\parallel}+\frac{\mathbf{E}\times\mathbf{B}}{B^2}=\begin{pmatrix}-\dfrac{I}{rRB^2}\dfrac{\partial\Phi}{\partial\theta}\\ \dfrac{KB_p}{n}\\ \dfrac{KB_\zeta}{n}-\dfrac{1}{B_p}\dfrac{\partial\Phi}{\partial r}\end{pmatrix},\tag{3}$$

where Φ is the electrostatic potential,

$$K=\frac{nV_p}{B_p},\tag{4}$$

corresponding to the poloidal flow, and

$$I=R^2\mathbf{B}\cdot\boldsymbol{\nabla}\zeta.\tag{5}$$

The toroidal symmetry is utilized in this description. The parallel component and averaged poloidal component of the momentum balance, Eq. (2), are given to be

$$-\frac{nI}{KB^2rR}\frac{\partial\Phi}{\partial\theta}\frac{\partial}{\partial r}\left[\frac{1}{2}\left(\frac{KB}{n}\right)^2\right]+\frac{B_p}{r}\frac{\partial}{\partial\theta}\left[\frac{1}{2}\left(\frac{KB}{n}\right)^2\right]+\frac{IB_\zeta}{B^2rR}\frac{\partial\Phi}{\partial\theta}\frac{\partial}{\partial r}\left[\frac{I}{RB_pB_\zeta}\frac{\partial\Phi}{\partial r}\right]-\frac{KB_pB_\zeta}{nr}\frac{\partial}{\partial\theta}\left[\frac{I}{RB_pB_\zeta}\frac{\partial\Phi}{\partial r}\right]$$

$$= -\frac{B_p}{m_i r}\frac{\partial}{\partial\theta}\left(\frac{\langle p_e\rangle}{\langle n\rangle}\ln n + \frac{5}{2}\frac{\langle p_i\rangle}{\langle n^{5/3}\rangle}n^{2/3}\right) - \frac{1}{m_i n}(\mathbf{B}\cdot\nabla\cdot\overleftrightarrow{\pi}_i)_{\text{bulk}} - \frac{1}{m_i n}(\mathbf{B}\cdot\nabla\cdot\overleftrightarrow{\pi}_i)_{\text{shear}}, \tag{6}$$

$$\left\langle -\frac{nI}{KB^2rR}\frac{\partial\Phi}{\partial\theta}\frac{\partial}{\partial r}\left[\frac{1}{2}\left(\frac{KB_p}{n}\right)^2\right] + \frac{B_p}{r}\frac{\partial}{\partial\theta}\left[\frac{1}{2}\left(\frac{KB_p}{n}\right)^2\right]\right\rangle = \frac{1}{m_i}\left\langle\frac{JB_pB_\zeta}{n}\right\rangle - \frac{1}{m_i}\left\langle\frac{\mathbf{B}_p\cdot\nabla\cdot\overleftrightarrow{\pi}_i}{n}\right\rangle_{\text{bulk}} - \frac{1}{m_i}\left\langle\frac{\mathbf{B}_p\cdot\nabla\cdot\overleftrightarrow{\pi}_i}{n}\right\rangle_{\text{shear}}, \tag{7}$$

where $\langle\ \rangle$ denotes the flux-surface average. The radial flow is taken into account, so the $\partial\Phi/\partial\theta$ terms are involved in the left side of Eqs. (6) and (7). Using the viscosity tensor $\overleftrightarrow{\pi}_i = (p_\parallel - p_\perp)(\hat{b}\hat{b} - \overleftrightarrow{\iota}/3)$, where $(p_\parallel - p_\perp)$ is the pressure anisotropy, $\hat{b}$ is the unit vector parallel to the magnetic field, and $\overleftrightarrow{\iota}$ is the unit tensor, the bulk viscosity term can be written as

$$(\mathbf{B}\cdot\nabla\cdot\overleftrightarrow{\pi}_i)_{\text{bulk}} = \frac{2}{3}\frac{B_p}{r}\frac{\partial}{\partial\theta}(p_\parallel - p_\perp) - (p_\parallel - p_\perp)\frac{B_p}{B}\frac{1}{r}\frac{\partial B}{\partial\theta}. \tag{8}$$

The first term of Eq. (8) is dominant, so only this term is kept in Eq. (6) hereafter. In contrast, the surface average is taken in Eq. (7), in which the second term of Eq. (8) remains. The pressure anisotropy, deduced from the drift kinetic equation with mass flow velocity, is [29]

$$p_\parallel - p_\perp = -2\sqrt{\pi}I_{ps}Km_iv_{ti}B\left(\frac{\partial}{\partial\theta}\ln B - \frac{2}{3}\frac{\partial}{\partial\theta}\ln n\right). \tag{9}$$

The integral I_{ps} is

$$I_{ps} = \frac{1}{\pi}\int_0^\infty dx x^2 e^{-x}\int_{-1}^{1} d\eta\left(\frac{1}{2} - \frac{3\eta^2}{2}\right)^2\frac{y/\sqrt{x}}{U_t^2 + (y/\sqrt{x})^2}, \tag{10}$$

where

$$y = \frac{r\nu_T B}{v_{ti}B_p}, \tag{11}$$

$$U_t = G_r\left[\eta + \left(-\frac{E_r}{B} + V_\parallel\frac{B_p}{B}\right)\Big/\left(\sqrt{x}\frac{v_{ti}B_p}{B}\right)\right], \tag{12}$$

ν_T is the characteristic collision frequency defined in Ref. 30, and G_r is a geometric factor, taken to be $G_r = 1$ in this paper. The shear viscosity is given by the second perpendicular derivative of the flow velocity, and is here simply given to be

$$(\mathbf{B}\cdot\nabla\cdot\overleftrightarrow{\pi}_i)_{\text{shear}} = -m_in\mu\mathbf{B}\cdot\nabla_\perp{}^2\mathbf{V}, \tag{13}$$

where μ is a shear viscosity coefficient. The coefficient μ depends on the radial electric field and has spatial variation, but we consider it to be constant in space for simplicity. This is because we are focusing on the structural formation mechanism from the nonlinearity of viscosity terms. The structural formation mechanism from turbulent induction will be treated elsewhere. The Boltzmann relation

$$n = \bar{n}\exp\frac{e\Delta\Phi}{T_i} \tag{14}$$

is adopted here to determine variables, where $\bar{f}$ and Δf represent the spatial average and perturbed parts of quantity f, respectively. The variables that must be determined from Eqs. (6), (7), and (14) are K, Φ, and n, which have the radial and poloidal variations. A variable

$$\chi = \ln(n/\bar{n}) \tag{15}$$

is introduced to represent density variation. From the Boltzmann relation, Eq. (14), χ is directly related to the potential perturbation.

B. Ordering and iterative process for solving equations

In this paper, we are mainly concerned with the case in which the poloidal Mach number $M_p \sim 1$, and a steep structure in the poloidal direction is formed in this case, so the shock ordering, which is

$$\chi = O(\varepsilon^{1/2}), \tag{16}$$

is adopted where ε is the inverse aspect ratio. The calculation is carried out only near the edge in a large aspect ratio tokamak, so ε is taken to be small. A condition

$$V_r/V_p \ll 1 \tag{17}$$

is satisfied, even if a strong poloidal shock exists. This condition is confirmed, *a posteriori*, by the derived structures. Condition $V_r/V_p \ll 1$ makes the model equation simpler. The continuous equation in a steady state

$$\text{div}(n\mathbf{V}) = 0 \tag{18}$$

shows K is a flux-surface variable. Expanding Eq. (6) with χ, and taking up to $O(\varepsilon)$, the following model equation is obtained:

$$-\hat{\mu}r^2\frac{B_0}{B_p}\frac{\partial^2}{\partial r^2}\{M_p\exp(-\chi) - E\} + \frac{2}{3}D\exp(-\chi)\frac{\partial^2\chi}{\partial\theta^2} + (1 - M_p{}^2)\frac{\partial\chi}{\partial\theta} + 2A\frac{\partial\chi^2}{\partial\theta} = \varepsilon\left(\left\{D - \hat{\mu}\frac{B_0}{B_p}\left[2r^2\frac{\partial^2 M_p}{\partial r^2} + 2r\frac{\partial}{\partial r}(M_p + E) - (M_p + E)\right]\right\}\times\cos\theta - 2M_p{}^2\sin\theta\right), \tag{19}$$

where

$$M_p = \frac{KB_0}{\bar{n}v_{ti}C_r}, \tag{20}$$

$$\hat{\mu} = \frac{\mu}{rv_{ti}C_r}, \tag{21}$$

$$A = \frac{M_p{}^2}{2} + \frac{5}{36C_r{}^2}, \tag{22}$$

$$C_r^2 = \frac{1}{2}\left(\frac{5}{3} + \frac{T_e}{T_i}\right), \tag{23}$$

$$D = \frac{4\sqrt{\pi} I_{ps} K B_0}{3\bar{n} v_{ti} C_r^2}, \tag{24}$$

and

$$E = \frac{I}{v_{ti} B_0 B_p C_r R} \frac{\partial \Phi}{\partial r}. \tag{25}$$

If flux surface average of the toroidal flow is zero, Eq. (3) gives

$$\frac{\partial \Phi}{\partial r} = \frac{K B_0 B_p}{\bar{n}}, \tag{26}$$

and substituting Eq. (26) into Eq. (25) gives

$$E \sim M_p. \tag{27}$$

This is the case with a strong toroidal damping, and M_p is proportional to the radial electric field in this case. The model equation (19) is simplified to be

$$\begin{aligned} &-\hat{\mu} r^2 \frac{B_0}{B_p} \frac{\partial^2}{\partial r^2}\{M_p[\exp(-\chi) - 1]\} + \frac{2}{3} D \exp(-\chi) \frac{\partial^2 \chi}{\partial \theta^2} \\ &\quad + (1 - M_p^2) \frac{\partial \chi}{\partial \theta} + 2A \frac{\partial \chi^2}{\partial \theta} \\ &\quad = \varepsilon\left(\left\{ D - \hat{\mu} \frac{B_0}{B_p}\left[2r^2 \frac{\partial^2 M_p}{\partial r^2} + 4r \frac{\partial}{\partial r} M_p - 2M_p \right]\right\}\right. \\ &\quad \left. \times \cos\theta - 2M_p^2 \sin\theta \right). \end{aligned} \tag{28}$$

In this paper, structural formation mechanism with a large poloidal flow is a much paid attention, so the strong toroidal damping condition is taken hereafter.

Now Eqs. (7), (14), and (28) determine the two-dimensional structure. This set of equations is solved as follows. A profile of M_p is obtained by solving Eq. (7) independently from Eq. (28). Equation (7) is the same as the equation used for obtaining a radial profile of the radial electric field in the previous H-mode transition models.[3,4,11] Then M_p (including the radial profile) is put into Eq. (28), and the two-dimensional structure of χ is obtained. Finally, the radial velocity is deduced.

Using these model equations, analysis is carried out in the region near the plasma edge, $r=(a-d)\sim a$, where $r=a$ is the position of the last closed flux surface. We consider the case in which the strong radial electric field is self-organized in the middle region of this domain (such as in the edge barrier or biased region), and chosen boundary condition is $\chi=0$ at $r=(a-d)$ and a. This is an idealization, considering that no perturbation exists outside of this region.

Equation (28) includes characteristic structures both in the radial and poloidal directions. These structures are coupled with the shear viscosity. Properties of the characteristic structures explained with the one-dimensional structure problem in the radial direction[13] are derived from setting $\mu = 0$.

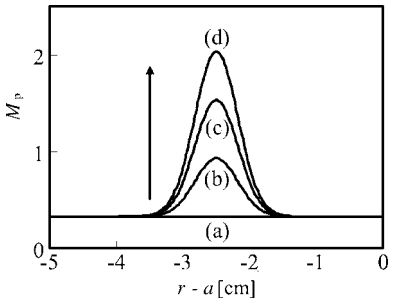

FIG. 1. Solitary radial structures of the radial electric field (translated into M_p) in electrode biasing driven H mode. The positions $r-a=-5$ and 0 cm are where the electrode and the limiter are placed, respectively. Increase of the maximum of M_p from plot (a) to (d) simulates the electrode driven L- to H-mode transition as in Fig. 2.

III. TWO-DIMENSIONAL STRUCTURE ON *L*/*H* TRANSITION

At the onset of L/H transition, the radial electric-field structure changes from homogeneous one to peaked one. A solitary M_p profile is shown in Fig. 1. This solitary profile is a solution of Eq. (1) with electrode biasing, which induces externally driven current.[11] This profile is typical in H mode driven by electrode biasing, having an electric field with a large magnitude and a large gradient as in spontaneously established H mode. A positive radial electric-field profile is also observed in the H-mode edge barrier with electron cyclotron heating.[31] Equation (28) is solved with this M_p profile to obtain two-dimensional structures of the electrostatic potential in H mode.

In L mode, the radial electric field is weak and the profile is rather flat. Figure 2(a) shows a χ profile, which is the logarithm of the density perturbation, when $M_p=0.33$ and $\mu=1.0\ \mathrm{m}^2/\mathrm{s}$. The potential perturbation is set to zero at the boundary $r-a=0, -5$ cm. The calculations are performed using the following parameters: $R=1.75$ m, $a=0.46$ m, $B_0=2.35$ T, $T_i=40$ eV, and $I_p=200$ kA. This profile shows gentle variation both in the radial and poloidal directions. The value $M_p=0.33$ is used as that for the state just before the L/H transition. Weak but constant radial electric field exists, so the potential difference between the boundaries is about 130 V in this case. The ratio $\Delta\Phi/\Phi$ is about 6% at the maximum of the potential perturbation.

For the H mode, Figs. 2(b)–2(d) show the χ profiles in accordance with the change of the M_p profile shown in Fig. 1. The region where M_p has a large value is localized in the middle of the shear region, so the density perturbation becomes large in this region. The magnitude of the perturbation increases as the magnitude of M_p increases.

Figures 3(a) and 3(b) show the profiles of the poloidal electric field calculated from Figs. 2(a) and 2(d), respectively, using Boltzmann relation, Eq. (14). A localized large poloidal electric field exists near the shock positions with large M_p in the H mode. In addition, the magnitude of M_p varies in the radial direction, so the poloidal position of the shock varies in the radial direction accordingly.

Shear viscosity μ controls the strength of the coupling between the poloidal shock and the radial solitary structure.[15]

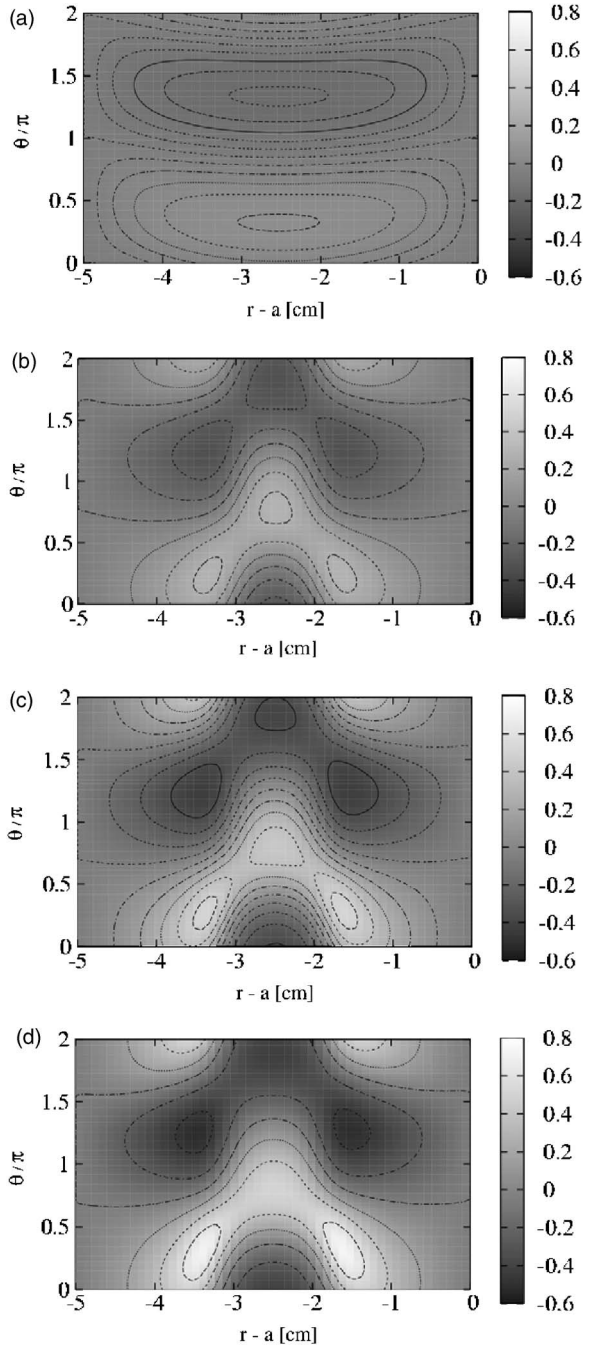

FIG. 2. Two-dimensional structures of the logarithm of the density perturbation. The M_p profiles are changed from spatially constant one (a) to peaked one (d), corresponding to those shown in Fig. 1.

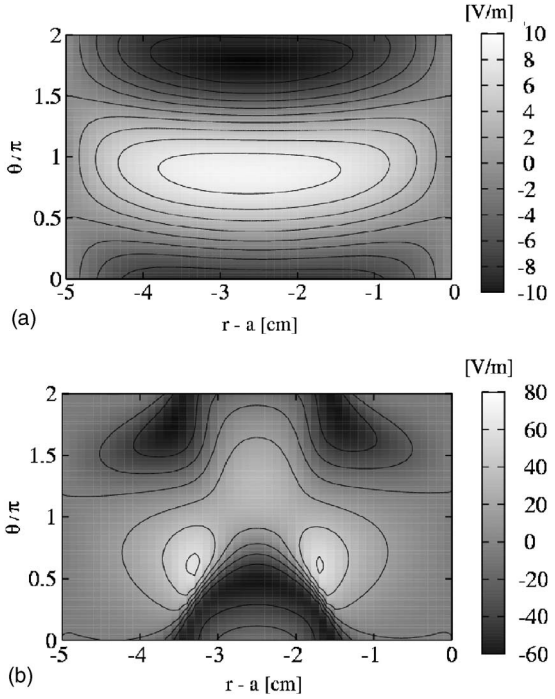

FIG. 3. Two-dimensional structures of the poloidal electric field with (a) the weak homogeneous E_r (L mode) and (b) the strong inhomogeneous E_r (electrode biasing driven H mode). These are obtained from Figs. 2(a) and 2(d), respectively.

If the radial coupling is weak, the strong shock is formed in every flux surface except near the boundaries. When the shear viscosity is very strong, no strong shock appears. In the intermediate case when the shear viscosity term and the poloidal derivative term are comparative, a structure with rather weak poloidal variation (weaken shock structure) is formed, and the maximum magnitude of that structure is inversely proportional to μ. Experimentally μ is estimated to be around 10^0 m^2/s from transport analysis on compact helical system[32] (CHS) or from the peak position of the radial electric field in electrode biasing H mode on Tokamak Experiment for Technology Oriented Research (TEXTOR).[33] Therefore, the plasmas in experimental devices are expected to be in the intermediate region. We use $\mu=1$ m^2/s in this calculation.

Comparison between the strong inhomogeneous E_r case and the weak homogeneous E_r case clarifies the formation of the localized steep two-dimensional structure. The strong E_r case has an E_r profile with a peak in the middle of the calculated region, although the weak E_r case has a spatially constant profile. The strong E_r case has a large potential perturbation (the maximum value $\delta\Phi_{\max}=50$ V in this case), and a large localized poloidal electric field in which the poloidal flow shear is strong (the maximum value $E_{p\,\max}=63$ V/m. This large poloidal electric field generates a large $E\times B$ flow pointing in the radial direction (the maximum value $V_{r\,\max}=28$ m/s. In the weak E_r case, the values are $\Delta\Phi_{\max}=4$ V, $E_{p\,\max}=9$ V/m, and $V_{r\,\max}=4$ m/s, respectively, which are one order smaller than in the strong E_r case. We conclude that the two-dimensional structure of the edge transport barrier exists and influences the plasma flow, for the plasma parameters that are relevant to the H-mode confinement.

IV. CONVECTIVE PARTICLE FLUX

Self-generation of the two-dimensional structure with the large shear $E\times B$ flow has great impact on the formation of the density pedestal in the transport barrier. Increase of particle transport on L/H transition is shown in this section.

To estimate the effect from the two-dimensional structural formation, we calculate the flux-surface-averaged flux in the radial direction as

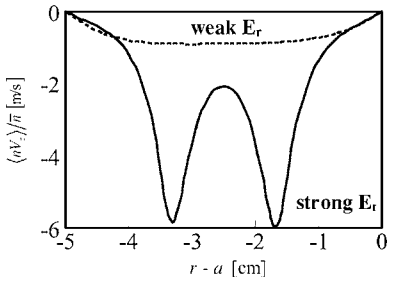

FIG. 4. Radial profiles of the flux-surface-averaged particle flux in the case of the weak homogeneous and strong inhomogeneous radial electric fields.

$$\langle nV_r \rangle = \left\langle n\frac{E_p}{B} \right\rangle = \frac{\bar{n}}{2\pi r}\frac{T_i}{eB_0}\int \frac{\partial}{\partial\theta}\left[\exp\left(\frac{e\Delta\Phi}{T_i}\right)\right] \times (1+\varepsilon\cos\theta)^2 d\theta \tag{29}$$

by using the two-dimensional solution obtained in Sec. III. The region with a large radial flow is localized, and the flow changes its direction at each poloidal position corresponding to the sign of the poloidal electric field, as shown in Fig. 3. The flux-surface-averaged flux indicates the net particle transport between different flux surfaces. Figure 4 represents the radial profiles of the flux-surface-averaged radial flux in the strong and weak E_r case. The radial flux has a negative value, so it points inward to the plasma center in this case. In the strong E_r case, not only the large magnitude of the poloidal flow but also the gradient and curvature of the poloidal flow increase the radial convective velocity. This enhancement of the velocity is derived from the form of the shear viscosity term in Eq. (13) that combines the poloidal asymmetry of magnetic field B with the gradient and curvature of the flow velocity. Figure 4 shows that the radial flux has maximum in the radial position where poloidal flow shear is larger.

The analysis of the two-dimensional structure reveals the existence of the inward particle pinch flow arising from poloidal asymmetry in tokamaks. This finding has a large impact on the transport. Figure 5 shows the relationship between the maximum of M_p and the particle pinch velocity. A moderate inward pinch velocity $V_r \sim 1$ m/s exists even in the weak E_r case (like the L mode). This velocity is equivalent to that observed in experiments. In the strong E_r case, which is relevant to the H mode or biased electrode experiments, a larger radial flow (inward pinch) is induced. The M_p profiles used to calculate Fig. 5 are the same as those shown in Fig. 1, and the increase in the maximum of M_p from 0.3 to 2.0 corresponds to the transition of the E_r structure from flat one to peaked (solitary) one. The increase of the maximum of M_p leads to an increase of the inward convective particle flux.

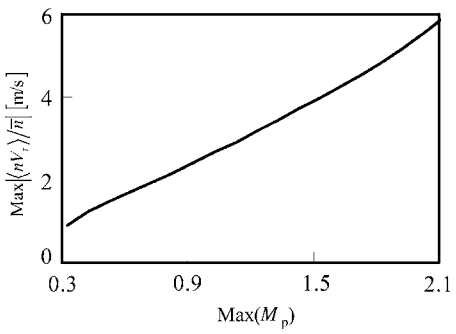

FIG. 5. Relationship between the maximum of M_p and the particle pinch velocity. Increase of the maximum of M_p corresponds to increase of the peak height of M_p, as shown in Fig. 1.

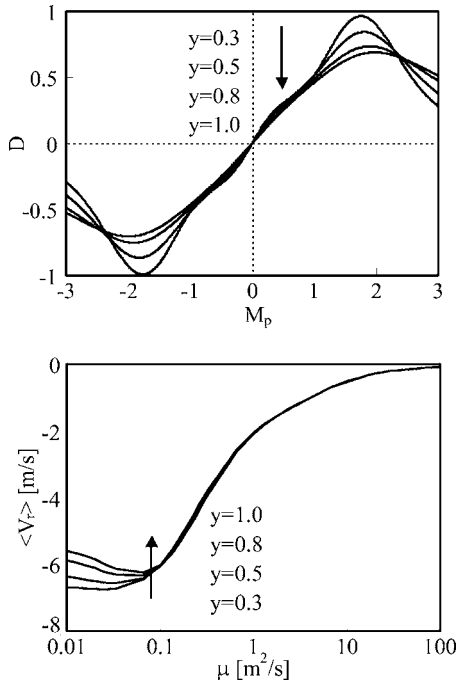

FIG. 6. (a) M_p dependence on coefficient D and (b) averaged convective velocity dependence on shear viscosity coefficient μ with the M_p profile given in Fig. 1(d). The cases with collision frequency $y=0.3-1.0$ are plotted to show the effect of collisionality.

V. EFFECT OF COLLISION

Collisionality is the important factor to describe the plasma condition near the edge region. We discuss the effect of collision on the two-dimensional structure in H mode in this section. Hard transition to the large E_r state is taken place in the plateau regime,[4] so the collision frequency in the plateau regime is considered here.

The transitions shown in the previous sections are for the case with $y=0.5$, where collision frequency y is defined in Eq. (11), and $y=1.0$ gives the boundary collision frequency between the plateau and Pfirsch-Schlüter regime. The collision frequency affects the two-dimensional structure through the function I_{ps} defined by Eq. (10), which represents the radial electric-field dependency of the pressure anisotropy. The coefficient D in Eq. (28) includes I_{ps}, and determines the steepness and position of the shock. Figure 6(a) shows the M_p dependence of coefficient D. The profile of coefficient D has a peak at $M_p \sim 1.8$ when the collision frequency is small, and the peak becomes smaller and broader as the collision frequency increases. Figure 6(b) shows the radial convective velocity dependency on the collisionality when the M_p profile is given as in Fig. 1(d). The absolute value of the convective velocity decreases as the collision frequency in-

creases with small $\mu(\mu<0.1\ \mathrm{m}^2/\mathrm{s})$, but for the realistic case when $\mu\sim 1\ \mathrm{m}^2/\mathrm{s}$, collisionality does not affect the convective velocity. The steepness of the shock changes in accordance with collisionality, but it affects little on the radial particle flux. This is because the poloidal position of the shock is influenced little by the value of D. The large convective flow in this regime is derived from the deviation of the peak position of the density and potential from that of $1/B$ that has $\cos\theta$ dependence. In other words, the phase difference between the density and the magnetic field gives the averaged flux. Therefore, the velocity V_r is influenced little if the poloidal position of shock does not change. The case with $\mu\sim 1\ \mathrm{m}^2/\mathrm{s}$ is intermediate for shock formation. The insensitiveness of the poloidal position of the shock on D is owing to the large flow shear and curvature. With large flow shear and curvature, the $\partial^2 M_p/\partial r^2$ term and the $\partial M_p/\partial r$ term are dominant, and D is negligible in the right-hand side of Eq. (28), so the collisionality does not have significant effect to change the position of the shock. Of course, the collisionality affects the radial electric-field transition. The transition to solitary solutions becomes harder to take place in the collisional case than in the collisionless case,[34] so this has a secondary effect for the two-dimensional structural formation.

VI. DIRECTION OF THE CONVECTIVE PARTICLE FLUX

There are some components that change the direction of the convective particle flux. Those are the poloidal Mach number M_p (radial electric field), the toroidal magnetic field, and the plasma current. In the previous sections, the cases with the positive radial electric field are discussed. When the radial electric field is negative as in spontaneous H modes, the shock changes its direction, so the convective velocity is inverted to direct outward.

The model equation (28) has two kinds of terms that show different response for inversion of the toroidal magnetic field and the plasma current. The shear viscosity terms that include μ do not change the direction of the convective velocity by the inversion of the toroidal magnetic field and the plasma current. On the contrary, the other terms change the direction by the inversion. In L and H modes, the shear viscosity and shock term are dominant, respectively, so in H mode the convective velocity tends to change its direction by the inversion of the toroidal magnetic field and the plasma current, but in L mode it does not. Taking account of these three components, in spontaneous H mode with a negative radial electric field, when the toroidal magnetic field and the plasma current point to the same and different directions, the convective velocity directs outward and inward, respectively.

VII. PEDESTAL FORMATION IN THE EDGE TRANSPORT BARRIER

The generation of the convective particle flux has a large impact on the pedestal formation after the onset of the L/H transition. The time evolution of the density is described by the particle conservation equation

$$\frac{\partial n}{\partial t} = -\nabla(n\mathbf{V} - D_a \nabla n) + S, \tag{30}$$

where D_a is a transport coefficient and S is a particle source. On the L/H transition, the suppression of turbulence and the reduction of diffusive transport occur in the transport barrier. The reduction of the diffusion coefficient explains the steepening of the H-mode pedestal in a final steady state, but the time constant of the pedestal formation is difficult to explain. The order estimation using Eq. (30) shows that the necessary time for reaching the final steep gradient in the region with the width δ is given by $\tau=\delta^2/D_a$ with reduced D_a in the H mode. It takes a longer time to form the pedestal ($\tau=25$ ms when $\delta=5$ cm and $D_a=0.1\ \mathrm{m}^2/\mathrm{s}$). It is known, however, the H-mode pedestal can be formed in a much shorter time $\tau \ll 10$ ms.[20]

Our analysis shows that abrupt change of the convective transport occurs simultaneously with the abrupt change of the M_p profile in the transport barrier region on the L/H transition. That is, if the convective velocity increases abruptly, the pedestal gradient increases, without delay, linearly in time, and the time constant of establishing the pedestal is shorten to be $\tau=\delta/V_r$ ($\tau=5$ ms when $\delta=5$ cm and $V_r=10$ m/s). Thus, the sudden increase of the convective flux is a new candidate for the cause of the rapid H-mode pedestal formation.

The first term of the right-hand side of Eq. (30) is the divergence of the particle convective flux. It must be pointed out that the divergence of the flux is important because it leads the density to change in a short time. The convective transport arising from the two-dimensional structure directs either inward or outward, depending on the sign of the electric field and the magnetic field. Nevertheless, both cases have the positive and negative gradient regions in their radial flux profiles. The pedestal starts to grow in the region of the negative gradient $dV_r/dr<0$, where the density rapidly increases. The positions of the negative gradient differ between the positive and negative convective flux cases. That is, our model predicts that the sign of the radial electric field makes difference in the position where the density begins to rise right after the onset of the L/H transition. Note that the convective transport enforces particle redistribution to form the density pedestal in the shear region both in the positive and negative radial electric field cases. Of course, the particle source and the boundary condition are also important to determine the profile in the steady state. What is concluded from our analysis is that the convective transport generated from the two-dimensional structure induces the rapid formation of the density pedestal in H-mode plasmas. The self-consistent calculation of the long-time evolution of the barrier after the transition requires the solution of the transport equation together with Eqs. (6) and (7), and is left for the future studies.

VIII. SUMMARY

In summary, multidimensionality was introduced into the H-mode barrier physics in tokamaks. The radial steep structure in H mode and the poloidal shock structure with the

large poloidal flow were taken into account in a self-sustained system. The model equations with shear viscosity were derived. The one-dimensional model that has been used to study the L/H transition condition[7] is validated by this two-dimensional analysis. The two-dimensional structures can be calculated by giving M_p profiles. This iterative process gives good approximation. The radial solitary structure of the strong radial electric field was found to be associated with the poloidal shock structure for the parameters that are relevant to H-mode plasmas. The radial convective flux with a magnitude of O(1) m/s exists and increases in the H-mode transport barrier. The collisionality has little effect on the convective transport in the experimental condition. The direction of the convective flux can be changed with the inversion of the radial electric field, the toroidal magnetic field, and the plasma current. Sudden increase of derivative of the convective transport at the onset of the transition was predicted by this theory. This provides a new explanation of the rapid H-mode pedestal formation.

There are few measurements of the poloidal structure. In continuous current tokamak (CCT), the poloidal density profile was measured in electrode biasing H mode.[18] In this paper, it is also suggested that the positions where the density begins to rise on the onset of the L/H transition differ in accordance with the direction of the radial electric field, the toroidal magnetic field, and the plasma current. To the best of knowledge of the authors, there has been no systematic experimental approach to identify the ramp-up speed of the density pedestal with a detailed structure inside the H-mode transport barrier, including the precise determination of the initial location where the edge pedestal starts to grow. To test our theoretical results experimentally, detailed measurements of the density or the electrostatic potential with high temporal and spatial resolutions are necessary. Identification of asymmetry (up down or in out) will help to clarify the effect of two dimensionality.[15] It is well known that asymmetry in tokamaks affects the H-mode transition, such as the difference of power threshold for L/H transition with x-point topologies,[35] and of energy confinement[36] and edge localized mode (ELM) behavior[37] with the direction of neutral beam injection. Developing the study of multiple-dimensional effects in tokamaks will give new understandings of transition physics in magnetic confined plasmas.

ACKNOWLEDGMENTS

Authors acknowledge discussions with Professor S.-I. Itoh, Dr. M. Yagi, Professor A. Fukuyama, Professor Y. Takase, Professor Y. Miura, and Professor G. R. Tynan. This work is partly supported by the Grant-in-Aid for Specially-Promoted Research of MEXT (16002005), by the Grant-in-Aid for Scientific Research of MEXT (15360495), by the collaboration programs of NIFS and of RIAM of Kyushu University, and by Research Fellowships of the Japan Society for the Promotion of Science for Young Scientists

[1] K. Itoh, S.-I. Itoh, and A. Fukuyama, *Transport and Structural Formation in Plasmas* (IOP, Bristol, 1999).
[2] F. Wagner, G. Becker, K. Behringer *et al.*, Phys. Rev. Lett. **49**, 1408 (1982).
[3] S.-I. Itoh and K. Itoh, Phys. Rev. Lett. **60**, 2276 (1988); S.-I. Itoh and K. Itoh, Nucl. Fusion **29**, 1031 (1989).
[4] K. C. Shaing and E. C. Crume, Phys. Rev. Lett. **63**, 2369 (1989).
[5] S.-I. Itoh and K. Itoh, J. Phys. Soc. Jpn. **59**, 3815 (1990).
[6] H. Biglari, P. H. Diamond, and P. W. Terry, Phys. Fluids B **2**, 1 (1990).
[7] See reviews, e.g., K. Itoh and S.-I. Itoh, Plasma Phys. Controlled Fusion **38**, 1 (1996); K. H. Burrel, Phys. Plasmas **4**, 1499 (1997).
[8] R. J. Taylor, M. L. Brown, B. D. Fried, H. Grote, J. R. Liberati, G. J. Morales, P. Pribyl, D. Darrow, and M. Ono, Phys. Rev. Lett. **63**, 2365 (1989).
[9] R. R. Weynants, G. Van N Oost, G. Bertschinger *et al.*, Nucl. Fusion **32**, 837 (1992).
[10] K. Itoh, S.-I. Itoh, M. Yagi, and A. Fukuyama, Phys. Plasmas **5**, 4121 (1998).
[11] N. Kasuya, K. Itoh, and Y. Takase, Nucl. Fusion **43**, 244 (2003).
[12] A. Fujisawa, H. Iguchi, H. Sanuki *et al.*, Phys. Rev. Lett. **79**, 1054 (1997).
[13] K. C. Shaing, R. D. Hazeltine, and H. Sanuki, Phys. Fluids B **4**, 404 (1992).
[14] T. Taniuti, H. Moriguchi, Y. Ishii, K. Watanabe, and M. Wakatani, J. Phys. Soc. Jpn. **61**, 568 (1992).
[15] N. Kasuya and K. Itoh, Phys. Rev. Lett. **94**, 195002 (2005).
[16] W. M. Stacey, Phys. Plasmas **9**, 3874 (2002).
[17] R. J. Taylor, P. Pribyl, G. R. Tynan, and B. C. Wells, *Proceedings of 15th International Conference on Plasma Physics and Controlled Nuclear Fusion Research, Seville, 1994* (IAEA, Vienna, 1995), Vol. 2, p. 127.
[18] G. R. Tynan, J. Liberati, P. Pribyl, R. J. Taylor, and B. Wells, Plasma Phys. Controlled Fusion **38**, 1301 (1996).
[19] P. Gohil, Plasma Phys. Controlled Fusion **44**, A37 (2002).
[20] F. Wagner, F. Ryter, A. R. Field *et al.*, *Proceeedings of the Thirteenth International Conference on Plasma Physics and Controlled Nuclear Fusion Research, Washington, 1990* (IAEA, Vienna, 1991), Vol. 1, p. 277.
[21] J. E. Rice, J. L. Terry, J. A. Goetz *et al.*, Phys. Plasmas **4**, 1605 (1997).
[22] A. A. Ware, Phys. Rev. Lett. **25**, 916 (1970).
[23] R. K. Varma, Plasma Phys. Controlled Fusion **40**, 1999 (1998).
[24] S. Puri, Plasma Phys. Controlled Fusion **41**, L35 (1999).
[25] F. Jenko, Phys. Plasmas **7**, 514 (2000).
[26] X. Garbet, L. Garzotti, P. Mantica, H. Nordman, M. Valovic, H. Weisen, and C. Angioni, Phys. Rev. Lett. **91**, 035001 (2003).
[27] N. Kasuya, K. Itoh, and Y. Takase, J. Plasma Fusion Res. **6**, 283 (2004).
[28] K. C. Shaing, E. C. Crume, and W. A. Houlberg, Phys. Fluids B **2**, 1492 (1990).
[29] K. C. Shaing, Phys. Fluids B **2**, 2847 (1990).
[30] S. P. Hirshman and D. J. Sigmar, Nucl. Fusion **21**, 1079 (1981).
[31] G. S. Kirnev, S. A. Grashin, L. N. Khimchenko, N. N. Timchenko, and G. Van Oost, Czech. J. Phys. **51**, 1011 (2001).
[32] K. Ida and N. Nakajima, Phys. Plasmas **4**, 310 (1997).
[33] N. Kasuya, Ph.D. thesis, University of Tokyo, 2003.
[34] N. Kasuya, K. Itoh, and Y. Takase, Plasma Phys. Controlled Fusion **44**, A287 (2002).
[35] B. LaBombard, J. E. Rice, A. E. Hubbard *et al.*, Phys. Plasmas **12**, 056111 (2005).
[36] H. Shirai, M. Kikuchi, T. Takizuka *et al.*, Nucl. Fusion **39**, 1713 (1999).
[37] Y. Sakamoto, H. Shirai, T. Fujita, S. Ide, T. Takizuka, N. Oyama, and Y. Kamada, Plasma Phys. Controlled Fusion **46**, A299 (2004).